Effect of the stroke-to-bore ratio on the performance of a dual-piston free piston engine generator

Zhiyuan Zhang[a], Huihua Feng[a], Boru Jia[a]*, Zhengxing Zuo[a], Andrew Smallbone[b], Anthony Paul Roskilly[b]

[a] *School of Mechanical Engineering, Beijing Institute of Technology, Beijing 100081, China*

[b] *Department of Engineering, Durham University, Durham, DH1 3LE, United Kingdom*

** Corresponding author E-mail: boru.jia@bit.edu.cn Tel: +86 15811505365*

Abstract:

The free piston engine generator (FPEG) is considered as one of the next generation efficient energy conversion device because of its compact structure, high geometric power ratio and low pollution. This paper investigated the effect of stroke-to-bore (S/B) ratio on the system operation characteristics and engine performance, constructed a detailed numerical model in MATLAB/Simulink and verified the experimental data whose difference value could be controlled within 5%. The effect of five S/B ratios (0.84, 0.91, 0.99, 1.07 and 1.14) and three compression ratios (8,9 and 10) was analysed at a constant bore diameter. The simulation results indicated that the operation frequency increased from 28.2Hz to 48.3Hz when the S/B ratio decreased from 1.14 to 0.84. The highest indicated power is 4.1kW when the S/B ratio is 0.84 and the compression ratio (CR) is 10. While for high thermal efficiency and fuel economy design, larger S/B ratio and higher operating compression ratio should be selected while keeping the periodic energy input unchanged. The heat transfer loss decreased from 29.0% to 20.4% when the S/B ratio increased from 0.84 to 1.14. And in the long stroke, ignition position needs to lean back (from 6.8mm to 24.8 when S/B increased from 0.84 to 1.14) so as to keep the compression ratio unchanged under different S/B ratios.

Keywords: Free piston engine generator, stroke-to-bore ratio, operation characteristics, combustion, heat transfer, thermal efficiency.

Nomenclature

a	shape factor
A	piston area (m^2)
A_f	friction parameters
$A_{leakage}$	leakage area (m^2)
b	shape factor
B_f	friction parameters
c	load constant of the linear generator ($N/(m/s)$)
C	capacitance (F)
C_d	combustion duration (s)
C_D	discharge coefficient
d	cylinder diameter (mm)
d_0	reference cylinder diameter (mm)
E	average temperature of the lubrication at liner (℃)
ε	voltage across the generator (V)
f	overall scaling factor
F_f	mechanical friction force (N)
F_l	gas force from the left cylinder (N)
F_m	force output from the linear electric machine (N)
F_r	gas force from the right cylinder (N)
F_{sl}	gas force from the left scavenging pump (N)
F_{sr}	gas force from the right scavenging pump (N)
γ	ratio of heat capacities
h	heat transfer coefficient ($W/(m^2 \cdot K)$)
H_e	enthalpy of the exhaust air (J)
H_l	enthalpy of the air leak (J)
H_i	enthalpy of the intake air (J)
i	current of the circuit (A)
k_v	generator property ($V/(m/s)$)

K_v	friction parameter
L	inductance (H)
λ	fuel mass fraction burned (%)
m	moving mass of the mover with the pistons (kg)
m_{air}	in-cylinder gas mass (kg)
p	in-cylinder gas pressure (Pa)
p_0	reference pressure (Pa)
ϕ	magnetic flux (Wb)
p_l	left-cylinder gas pressure (Pa)
p_r	right-cylinder gas pressure (Pa)
p_s	pressure in scavenging pump (Pa)
p_{sl}	pressure in left scavenging pump (Pa)
p_{sr}	pressure in right scavenging pump (Pa)
Q_c	heat release from the combustion process (J)
Q_{ht}	heat transfer loss (J)
Q_{in}	energy input in one running cycle (J)
R	ideal gas constant ($\mathrm{J}/(mol \cdot K)$)
R_c	resistance of the circuit (Ω)
T	temperature of the in-cylinder gas (K)
T_0	air temperature in the scavenging pump (K)
θ_0	reference temperature (℃)
t_s	combustion start time (s)
T_w	average cylinder wall temperature (K)
U	internal energy of the in-cylinder gas (J)
v	piston velocity (m/s)
V	gas volume (m^3)
v_p	average piston velocity (m/s)
x	piston displacement (m)

1. Introduction

1.1 Background

The free piston engine generator (FPEG) is a new type of energy conversion device that uses linear electric generator driven by free piston engine to convert the chemical energy of fossil fuel directly into electric energy. The linear reciprocating motion is the most important characteristic compared with the traditional internal combustion engine. The FPEG has received a lot of attention from many researchers in recent years and is considered as one of the most promising energy conversion device because it is compact in structure without crank mechanism, low friction loss for the absence of significant piston side force, high geometric power ratio and reliability attributed to a compact structure and multi-fuel feasibility for its variable compression ratio [1-6].

The FPEG can be mainly divided into single-cylinder single-piston type according to its structure, *i.e.* single-piston type with a corresponding rebound device, dual-cylinder dual-piston type, and single-cylinder dual-piston type with two corresponding rebound devices located at both ends. However, regardless of the form of FPEG, it is generally necessary to start with the help of a linear motor, and gradually transition to stable power generation after the cold start process is completed. Therefore, current studies on FPEG mainly focus on the process of engine cold start and stable generation. In order to improve FPEG performance, it is necessary to find out the influence of important design parameters on the design stage and determine the appropriate selection range. However, it is difficult to study the influence of design parameters from an experimental perspective because lots of the designed FPEG prototypes designed in the literature have not reached the stable generation stage. Therefore, the influence of design parameters on the performance of the prototype is not sufficiently studied.

1.2 Literature review

1.2.1 FPEG simulation and experimental research

Pescara first proposed the concept of modern free piston engine around 1922 [7, 8], which was originally applied to air compressors and gas generators. In recent years, its

goal has been to output electrical and hydraulic energy, and different free piston engine generator prototypes have been designed by researchers around the world.

Nigel Clark et al. [9, 10] from West Virginia University (WVU) have been committed to the research of FPEG ignited by two strokes since 1998. The prototype they designed used air inlet injection and loop scavenging with a cylinder diameter of 36.5 mm and a maximum design stroke of 50.0 mm. The operating frequency of the system under test was 23.1Hz, and the maximum output power was 313W. However, the prototype was found to be difficult to start and was prone to misfire during operation. Houdyschell et al. [11, 12] designed a two-stroke compression ignition prototype in 2000, which used two motoring coils to start the free piston engine, but it was still difficult to achieve the cold start of engine. Starting in 2014, WVU researchers designed a new prototype to be used as a home-level Combined Heat and Power (CHP) generator. It is based on a two-stroke, gas-fuelled, spark-ignited single-cylinder engine assisted by a mechanical spring as a rebound device. The results indicated that an increase in spring stiffness from 50 to 350 kN/m improved the system operating frequency by 18% and power output by 12% under constant compression ratio, while the system efficiency decreased by 2%, which was attributed to the decrease of charging efficiency (EGR ratio increased by 12%) under the conditions of constant intake/exhaust and high frictional loss (4%) [13, 14].

Van Blarigan et al. [15] at Sandia National Laboratory (SNL) have done a lot of research on FPEG since the 1990s. Their prototype used Homogeneous Charge Compression Ignition (HCCI) combustion mode and a single-zone chemical dynamics model to study the performance of free piston engine. In 2002, they developed loop-scavenged system aiming to optimize the scavenging parameters and maximize performance. The results showed that the uniflow scavenging geometry with low intake pressure was able to achieve optimum engine efficiency and emission characteristics [16, 17]. They began to design the single-cylinder dual-piston FPEG prototype in 2008, and have done a lot of work on the synchronous operation of piston, thermodynamic response characteristics and engine compression ratio control. Leick et al. [18] designed a relative FPEG prototype to study its potential for hybrid vehicles. The simulation and

experimental results showed that typical power output of the linear generator was 16 to 19 kW and HCCI combustion with hydrogen of low equivalence ratio was successfully demonstrated. According to the simulation model, if the prototype could run at a frequency of 44 Hz, the electrical efficiency could reach 97.5%, which was difficult to achieve in the prototype due to the influence of friction.

Mikalsen and Roskilly [19-23] from Newcastle University simulated and experimentally studied FPEG. They proposed a novel approach of the modelling of free piston engines using a coupled dynamic-multidimensional simulation model. The simulation results showed that the influence of TDC position and compression ratio on the performance of free piston diesel engines were greater than that of free piston petrol engines due to the great influence of gas movement in cylinder during combustion. Based on the basic operating characteristics of the single-piston free piston engine, a full-cycle simulation model was established and the control strategy of the single-piston free piston engine was studied. The results showed that it was feasible to control the dead center position in the full load range using fuel mass and air control variables captured in the bounce chamber. The influence of cyclic variation on engine operation was studied. The variation of peak gas pressure in cylinder was found to be significantly higher than that in conventional engines.

Researchers from Beijing Institute of Technology (BIT) simulated and experimentally studied the cold start of engine and stable generation and developed ignition and compression ignition prototypes [24, 26]. Boru Jia *et al.* proposed a detailed numerical model to investigate the characteristics of FPEG, and the simulation results agreed well with the test data from a running prototype [27]. The performance of engine during stable generation was predicted, and the efficiency was estimated to be 31.5% at a power output of 4 kW. The experimental results indicated that the peak in-cylinder pressure and compression ratio nonlinearly increased and became stable during the start of engine, the air fuel mixture was successfully ignited with a compression ratio of more than 9:1, and the peak in-cylinder pressure was up to 40bar after ignition [28, 29]. Researchers at Toyota designed a single-cylinder, single-piston FPEG prototype that ran continuously for a long period of time [30-32]. The spark ignition and the Premixed

Charged Compression Ignition (PCCI) combustion modes were simulated, and the results showed that by using the two combustion modes, the air fuel mixture could be successfully ignited, with an output power of up to 10kW. The linear electric machine was used to control the displacement of the free piston. The simulation and experimental results showed that the proposed control strategy could reduce the cyclical fluctuation caused by abnormal combustion.

At present, many experiments and simulation results of many research institutions indicate that free piston engine generator has great application prospects. However, the design of FPEG does not have certain criteria, and few articles mention the important effect of design parameters on the free piston engine's performance. Refer to the traditional internal combustion engine, S/B is also one of the important design parameters of the free piston engine.

1.2.2 The research on S/B ratio

The S/B ratio is one of the key parameters for the design of internal combustion engine, and lots of experimental and numerical work has been conducted to study its effect on engine performance. Siewert [33] studied the effect of S/B ratio on Indicated Specific Fuel Consumption (ISFC) and emissions of a gasoline spark-ignited single-cylinder engine with constant compression ratio and bore diameter. The experimental results showed that the ISFC and hydrocarbon increased significantly as S/B ratio decreased. The increase of cylinder heat loss led to the increase of combustion duration, which was considered to be the main reason for the increase of ISFC. The increased surface-to-volume ratio was the principal cause of the increase in hydrocarbon emissions. Filipi *et al.* [34] investigated the influence of the S/B ratio on the combustion, heat transfer and overall efficiency of a homogeneous charge spark ignition engine with a given displacement from a quasi-dimensional turbulent flame entrainment model. The influences of three typical S/B ratios (0.7, 1.0 and 1.3) were analysed, and the results showed that long stroke could reduce heat transfer loss and improve thermal efficiency (faster burning and smaller overall area of chamber walls), while these effects were found to be non-linear. The long-stroke engine exhibited better performance on braking

fuel economy at a low speed of engine, while friction loss gradually decreased at a high speed of engine.

Ozcan *et al.* [35] employed a quasi-dimensional multi-zone model to simulate a variable stroke length, liquefied petroleum gas fuelled, four-stroke engine. The simulation results showed that engine brake torque and power was improved using the variable stroke technique compared to the original engine design, and the emission characteristics were also improved. Ikeya *et al.* [36] improved the thermal efficiency of engine by increasing S/B ratio (ranging from 1.2 to 2.0), and the results showed a brake thermal efficiency of 45% was achieved at an engine speed of 2,000rpm with a S/B ratio of 1.5, a compression ratio of 17, an effective compression ratio of 12.5, and an EGR rate of more than 30%. Curto-Risso *et al*. [37] simulated the power output and the efficiency of a realistic Otto-like engine by a quasi-dimensional turbulent combustion engine. The simulation results showed that intermediate values between 0.6 and 0.8 give the most favourable results (about 18% better for power and 7% better for efficiency) and the optimum values of stroke-to-bore ratio minimize network losses in a wide speed interval.

The S/B ratio is one of the key parameters not only for the design of internal combustion engine, but also for the design of the free piston engine. However, during the design process of the free piston engine on this stage, S/B ratio is mostly chosen by direct reference to the reversing reciprocating engines of the same size. However, due to the differences in piston dynamics and system performance between FPEG and reciprocating engines, the current selection methods and analysis of FPEG S/B ratio cannot fully exploit the potential advantages of FPEG.

1.3 Aim and methodology

In this research, a detailed system numerical model of the FPEG was established. The effect of the S/B ratio on the performance of a dual-piston type free piston engine was investigated. The changes of indicated thermal efficiency, indicated power, indicated specific fuel consumption, heat transfer loss at different S/B ratio and different compression ratio were studied. Meanwhile, the comprehensive influence of S/B ratio

and compression ratio on the performance of free piston engine was analysed and discussed in this article, which is helpful to provide guidance for selecting the design parameters of PFEG prototype, and to provide appropriate boundaries for selecting engine compression ratio and ignition position.

2. FPEG configuration and the description of operating stroke in FPEG

2.1 FPEG configuration

The dual-piston two-cylinder FPEG has attracted much attention due to its compact structure, high power/weight ratio and multi-fuel feasibility. The author's group set up a dual-piston dual-cylinder spark ignition FPEG prototype and the schematic diagram is shown in Fig. 1. The linear electric machine is located in the middle of two free piston engines, and the driving force of motor is connected with two pistons by connecting rods and piston pins. The free piston engine adopts two-stroke thermodynamic cycle and the intake and exhaust process is completed by scavenging port and exhaust port. Fuel and intake air are mixed in the intake pipe, and then the mixture goes into the scavenge chamber. The fuel-air mixture is then ignited through the spark plug, and high-pressure gas drives the piston assembly, which converts mechanical energy into electrical energy by a linear generator.

The operating process of FPEG can be divided into two stages, *i.e.* the cold start of engine and stable generation. During the cold start of the engine, the linear motor as the motor drives the driving components to reciprocate in a straight line. The pistons connected with the motor driving unit compress the fuel-air mixture for ignition until the cod start is completed. Then, the linear electric machine is switched to its generating mode to generate electricity. This research mainly focuses on the system characteristics during stable generation. Please refer to the previous papers published by the author's group for the results during the cold start of engine [26,28-29].

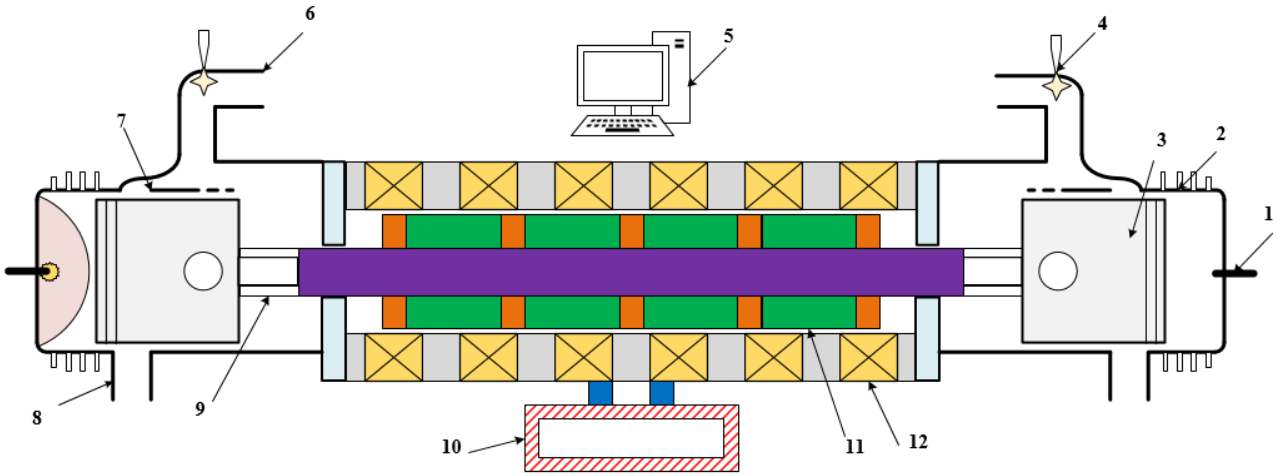

1. Spark plug 2. Cylinder 3. Piston 4. Fuel injector 5. Control system 6. Air-intake tube
7. Scavenging port 8. Exhaust port 9. The connecting rod 10. External load 11. Mover 12. Stator

Fig 1. Schematic diagram of FPEG configuration

2.2 The description of operating stroke in the FPEG

The design stroke of FPEG has an important effect on the performance of free piston engines as it can affect the dynamic characteristics of piston and gas exchange process. The limit distance that the piston can travel in the cylinder is defined as the design stroke, as shown in Fig. 2. The change of design stroke is achieved by changing the length of the connecting rod. Effective stroke refers to the actual operating stroke of the free piston from its bottom dead centre to its top dead centre. As the designed free piston engine adopts scavenging air passage, the effective compression stroke is the same under the condition of constant compression ratio. This is because the value of the compression ratio is theoretically equal to the effective compression stroke divided by the remaining stroke. In order to ensure the same compression ratio under different S/B ratios, the ignition position needs to be adjusted. The detailed parameters are listed in Table 1 when the S/B ratio is 1.14 and the operating compression ratio is 9.

Table 1 Detailed parameters of experimental prototype when S/B ratio is 1.14.

Specifications	Value	Unit
S/B ratio	1.14	—
Cylinder bore	52.5	mm
Design stroke	60	mm
Exhaust port position	0	mm
Intake port position	+5	mm
Mass of the mover assembly	5	kg
Operating frequency	9	—
Effective stroke	54	mm
Effective compression stroke	27	mm
Remaining stroke	3	mm

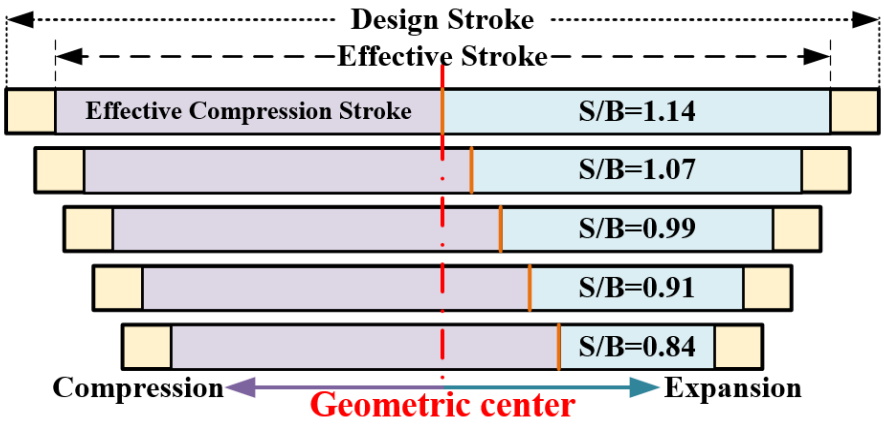

Fig 2. FPEG operation stroke and design stroke under different S/B ratios

3. Modelling and simulation

3.1 Numerical modelling

During the system stable generating process, the forces acting on the mover (which is the significant moving part of the FPEG and mainly include pistons, the mover of the linear machine and the connector between them) including in-cylinder gas forces, linear motor force, mechanical friction force and the inertial force of the moving parts. The

kinetic equation of the actuator can be derived from Newton's second law, as shown in Fig. 3.

$$m\frac{d^2x}{dt^2} = \overrightarrow{F_l} + \overrightarrow{F_r} + \overrightarrow{F_{sr}} + \overrightarrow{F_{sl}} + \overrightarrow{F_m} + \overrightarrow{F_f} \quad (1)$$

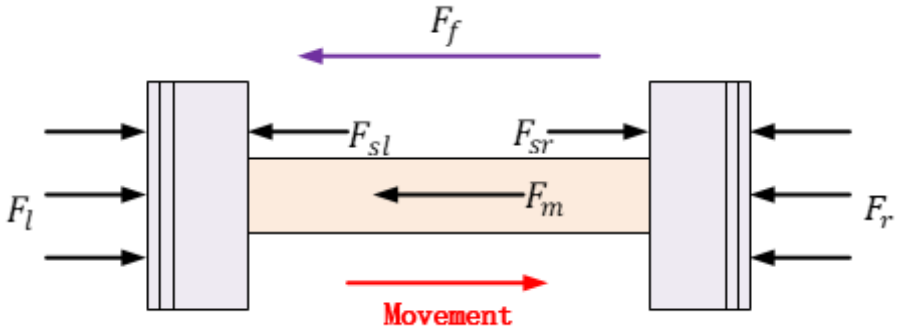

Fig 3. Dynamics of the mover

where m is the mass of the moving mover assembly (Unit: kg); x is the displacement of the mover (m); F_l is the gas force of left cylinder; F_r is the gas force of right cylinder (N); F_{sl} and F_{sr} is the gas force from the left and right scavenging pump (N); F_m is the force from the linear electric machine (N); F_f is the friction force (N).

The gas pressure is derived from the gas pressure and piston area:

$$F_l = p_l \cdot A;\ \ F_r = p_r \cdot A \quad (2)$$

$$F_{sl} = p_{sl} \cdot A;\ \ F_{sr} = p_{sr} \cdot A \quad (3)$$

where p_l and p_r is the left and right in-cylinder pressure (Pa); p_{sl} and p_{sr} is the left and right scavenging pump pressure (Pa); A is the section area of the piston (m^2).

3.1.1 In-cylinder thermodynamic sub-model

The actual change of in-cylinder pressure is complicated. Therefore, appropriate assumptions and simplifications were adopted in the modelling process. For example, the in-cylinder gas is considered as ideal gas, in-cylinder gas property is analysed based on a zero-dimensional thermodynamic approach while neglecting the kinetic energy and potential energy of the gas in the cylinder. According to the First Law of Thermodynamic, the equation of the in-cylinder gas energy change over time in a cylinder is:

$$\frac{dU}{dt} = -p\frac{dV}{dt} + \left(\frac{dQ_c}{dt} - \frac{dQ_{ht}}{dt}\right) + \sum_i \dot{H}_\iota - \sum_e \dot{H}_e - \sum_l \dot{H}_l \quad (4)$$

where U is the internal energy of the in-cylinder gas (J); V is the gas volume (m^3); Q_c is the heat release from the combustion process (J); Q_{ht} is the heat transfer loss (J); H_i is the enthalpy of the intake air (J) and H_e is the enthalpy of the exhaust air (J); H_l is the enthalpy of the air leak (J).

When the intake and exhaust outlets are closed, the enthalpy of intake and exhaust is zero, and the energy conservation equation is:

$$\frac{dU}{dt} = -p\frac{dV}{dt} + \left(\frac{dQ_c}{dt} - \frac{dQ_{ht}}{dt}\right) - \sum_l \dot{H}_l \tag{5}$$

Furthermore, the pressure change equation of the gas in the cylinder can be transformed into:

$$\frac{dp}{dt} = \frac{\gamma - 1}{V}\left(\frac{dQ_c}{dt} - \frac{dQ_{ht}}{dt}\right) - \frac{p\gamma}{m_{air}}\frac{dm_{air}}{dt} - \frac{p\gamma}{V}\frac{dV}{dt} \tag{6}$$

where p is the in-cylinder gas pressure (Pa); γ is the ratio of heat capacities; m_{air} is the mass of the in-cylinder gas (kg).

The time-based Wiebe function is used to modify the FPEG combustion process, and the mass fraction of combustion is expressed as:

$$\lambda = 1 - \exp\left(-a\left(\frac{t - t_s}{C_d}\right)^{b+1}\right) \tag{7}$$

$$\frac{dQ_c}{dt} = Q_{in}\frac{d\lambda(t)}{dt} \tag{8}$$

where λ is the mass fraction of fuel burned (%); a and b are shape factors; C_d is the combustion duration (s); t_s is the time when combustion starts (s); Q_{in} is the energy input in a running cycle (J). Therefore, the heat release during combustion can be expressed as:

$$\frac{dQ_c}{dt} = a\frac{b+1}{C_d}\left(\frac{t - t_s^b}{C_d}\right)exp\left(-a\left(\frac{t - t_s}{C_d}\right)^{b+1}\right)Q_{in} \tag{9}$$

Due to the temperature difference between gas and cylinder wall, heat transfer loss is inevitable. In this paper, the Hohenberg heat transfer equation is used to calculate the heat transfer [38]:

$$\dot{Q}_{ht} = hA_{cyl}(T - T_w) \tag{10}$$

$$\mathrm{h} = 130V^{-0.06}\left(\frac{p(t)}{10^5}\right)^{0.8} T^{-0.4}\left(v_p + 1.4\right)^{0.8} \tag{11}$$

where $\dot{Q}_{ht}$ is heat flow rate (J/s); h is the heat transfer coefficient ($\mathrm{W}/(m^2 \cdot \mathrm{K})$); A_{cyl} is the area of the cylinder wall in contact with the burned mas (m^2); T is the temperature of the in-cylinder gas (K); T_w is the average temperature of cylinder wall (K); v_p is the average speed of piston (m/s).

The variation of gas mass in the cylinder is mainly caused by leakage through the piston ring. The mas flow rate is determined by the thermodynamic properties of the in-cylinder gas, the difference in pressure between the in-cylinder gas and the scavenging pump and a reference air leakage area. The mass flow rate can be expressed as [39]:

$$\dot{m}_{air} = \frac{C_D \cdot A_{leakage}}{(RT_0)^{1/2}} p(t) \left[\frac{p_s}{p(t)}\right]^{1/\gamma} \left\{\frac{2\gamma}{\gamma - 1}\left[1 - \left(\frac{p_s}{p(t)}\right)^{(\gamma-1)/\gamma}\right]\right\}^{1/2} \tag{12}$$

where $\dot{m}_{air}$ is the mass flow rate of in-cylinder gas (kg/s); C_D is the discharge coefficient; $A_{leakage}$ is the leakage area (m^2); R is the ideal gas constant ($\mathrm{J}/(\mathrm{mol} \cdot \mathrm{K})$); T_0 is the air temperature in the scavenging pump (K); p_s is the air pressure in the scavenging pump (Pa); and if

$$\frac{p_s}{p(t)} \leq [2/(\gamma + 1)]^{\gamma/(\gamma-1)} \tag{13}$$

The equation of air mass flow rate equation:

$$\dot{m}_{air} = \frac{C_D \cdot A_{leakage}}{(RT_0)^{1/2}} p(t)\gamma^{1/2} \left(\frac{2}{\gamma + 1}\right)^{(\gamma+1)/2(\gamma-1)} \tag{14}$$

3.1.2 Linear electric generator sub-model

The linear electric machine operates as a generator during stable generation. The permanent magnet mover connected with the piston assembly cuts off the magnetic induction wire for generating electricity. The voltage across the generator ε in this process can be written as:

$$\varepsilon = R_c i + L\frac{di}{dt} + C\int idt \tag{15}$$

where R_c is the resistance of the circuit (Ω); i is the current (A); L is the inductance (H); C is the capacitance (F).

According to Faraday's law of electromagnetic induction, the back electromotive voltage is (assuming the load circuit is pure resistance circuit):

$$\varepsilon = N\frac{d\phi}{dt} = k_v\frac{dx}{dt} \tag{16}$$

where ϕ is the magnetic flux (Wb); k_v is a generator property (V/(m/s));

Finally, the load force of the linear electric generator can be written as:

$$F_m = -cv \tag{17}$$

where c is the load constant of the linear generator (N/(m/s)); v is the velocity of the mover (m/s).

3.1.3 Friction sub-model

The friction of FPEG mainly includes the friction between piston ring and cylinder and the friction of linear electric generator. Based on previous studies, empirical relations were used to calculate the parametric friction between ring and cylinder wall:

$$F_{fring/liner} = f\left[-sign(v)\cdot A_f\cdot\sqrt{|v|}\right]\left[1 - B_f\cdot\frac{E-\theta_0}{\theta_0}\right]\left[1 + K_v \cdot\frac{p(t)}{p_0}\right]\left(\frac{d}{d_0}\right) \tag{18}$$

where f is the overall scaling factor; A_f, B_f and K_v are friction parameters; E is the average temperature of the lubrication at liner (℃); θ_0 is reference temperature (℃); p_0 is reference pressure (bar); d is cylinder diameter (mm) and d_0 is reference cylinder diameter (mm).

3.2 Simulation method

A system-level model of a dual-cylinder type FPEG was established in MATLAB/Simulink to solve the numerical equations. The developed simulation model included the overall kinetics model and three important sub-models: in-cylinder gas force sub-model, linear electric generator sub-model and friction sub-model. The in-cylinder gas force sub-model consisted of six processes: intake, compression (expansion), ignition, exhaust, air leakage and heat transfer. The specific process is set in State flow in Simulink. The exhaust port and intake port position changes with the change of S/B ratio in the simulation model as shown in Table 2. The structural

parameters of the internal combustion engine and linear electric generator needed to be set in advance. The cylinder bore is one of the fundamental design parameters for the FPEG engine, and it was set to 52.5mm in this research. The S/B ratio was then determined by the value of design stroke, and the cylinder bore remained unchanged during simulation. Therefore, the operation characteristics and in-cylinder thermodynamic will change with the change of S/B ratio. The performance of the FPEG was investigated by the simulation results under different S/B ratios and the simulation model is shown in Fig. 4.

Table 2 Exhaust port and intake port position at different S/B ratio.

S/B ratio	Exhaust port position	Intake port position	Unit
0.84	+8	+13	mm
0.91	+6	+11	mm
0.99	+4	+9	mm
1.07	+2	+7	mm
1.14	0	+5	mm

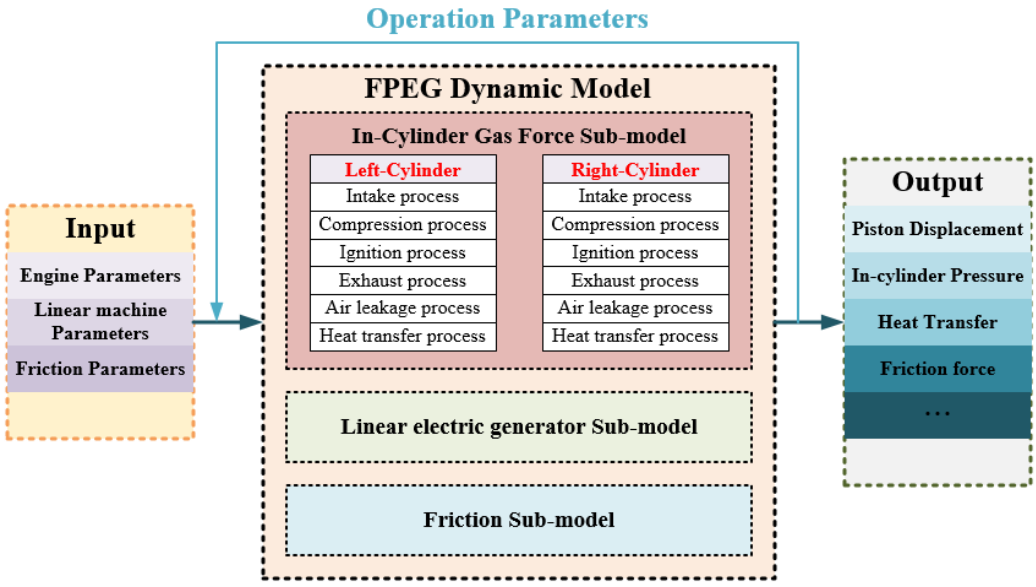

(a) The basic structure of the simulation model

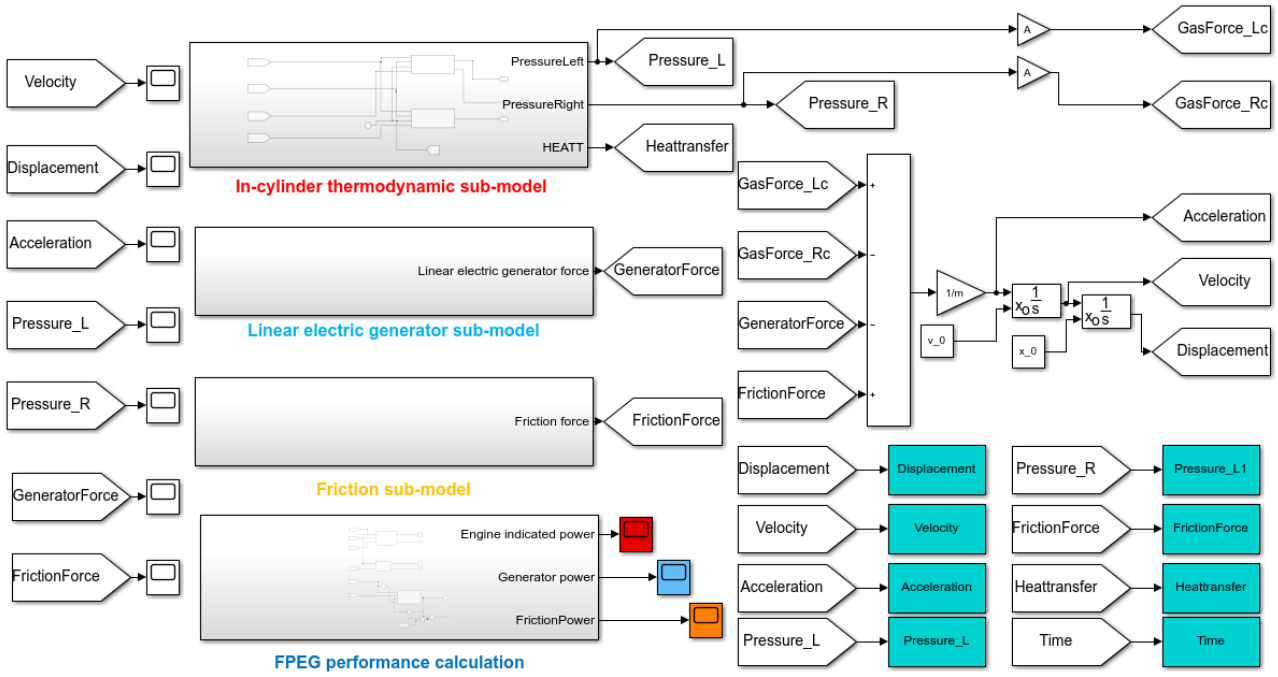

(b) The Simulink model in MATLAB

Fig 4. Diagram of the simulation model in MATLAB/Simulink

3.3 Model validation

The designed dual-piston dual-cylinder FPEG prototype is shown in Fig. 5. It is a spark ignited gasoline engine operating in a two-stroke thermodynamic cycle, and linear machine located at the middle of the two cylinders is permanent magnet tubular. The test bench consisted of a National Instruments PXIe data acquisition system, free piston engine and linear electric machine control system. The data acquisition system collected data from the displacement sensor, cylinder pressure sensor (Kistler 6052C31) and electrical power output (Yokogawa WT500), mass flow meter (Endress+Hauser). The control system ensured the continuous operation of the FPEG prototype, and output the triggered signals for ignition and injection system.

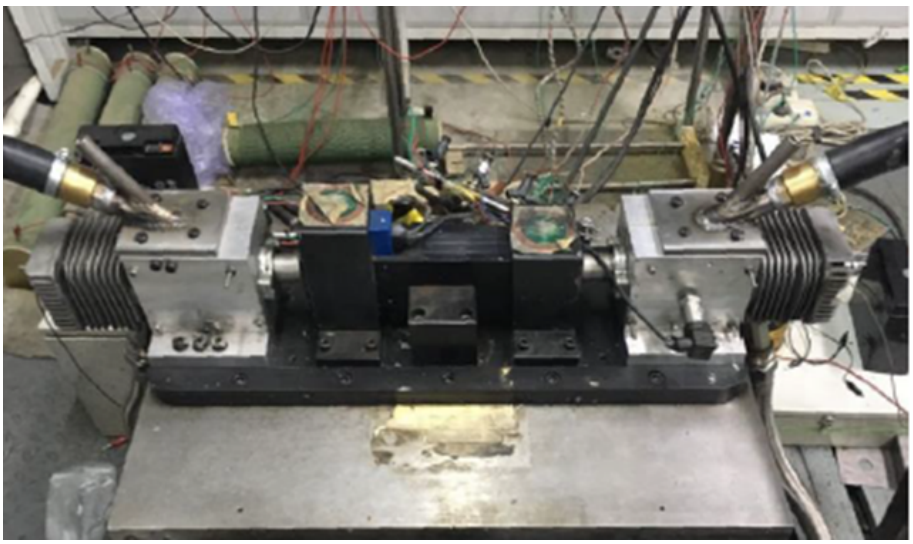

Fig 5. Prototype and test bench

The numerical model was validated with the experimental data from the prototype. Please refer to the previous publications published by the authors' group for more details on the numerical modeling and validation results [26, 28]. The difference between the simulated cylinder pressure and the experimental data could be controlled within 5%, indicating the accuracy of the model.

4. Results and discussion

4.1 Piston dynamics at different S/B ratios

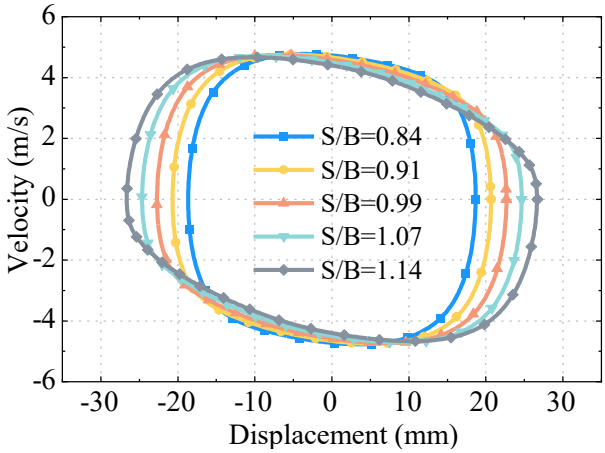

Fig 6. FPEG piston dynamics at different S/B ratios

The operating characteristics of FPEG with different S/B ratios are shown in Fig. 6. The compression ratio of engine was set to 9. It was found that the difference in the peak speed of the piston did not significantly change with the change of S/B ratio.

However, the unique operating characteristics of the free piston engine such as rapid expansion and slow compression became more prominent as the S/B ratio increased.

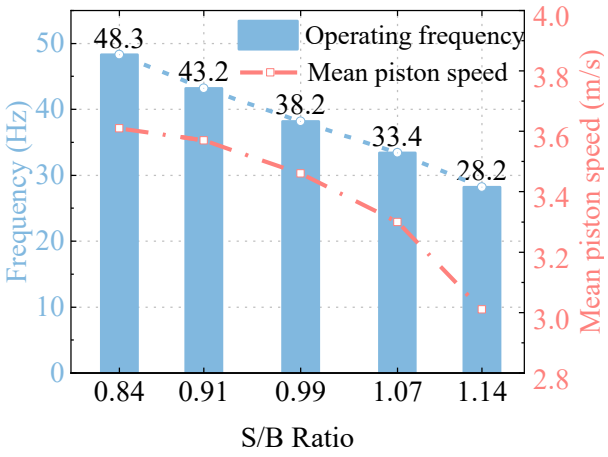

Fig.7 The operating frequency of the system and the mean speed of piston at different S/B ratios

The operating efficiency of the system and the mean speed of piston at different S/B ratios are shown in Fig. 7. The operating frequency of the system decreased from 48.3Hz to 28.2Hz as S/B ratio increased. With the increase of S/B, both design stroke and effective stroke increased, while the working compression ratio was fixed, so the mean speed of the piston decreased with the increase of S/B ratio.

4.2 Performance of free piston engine at different S/B ratios

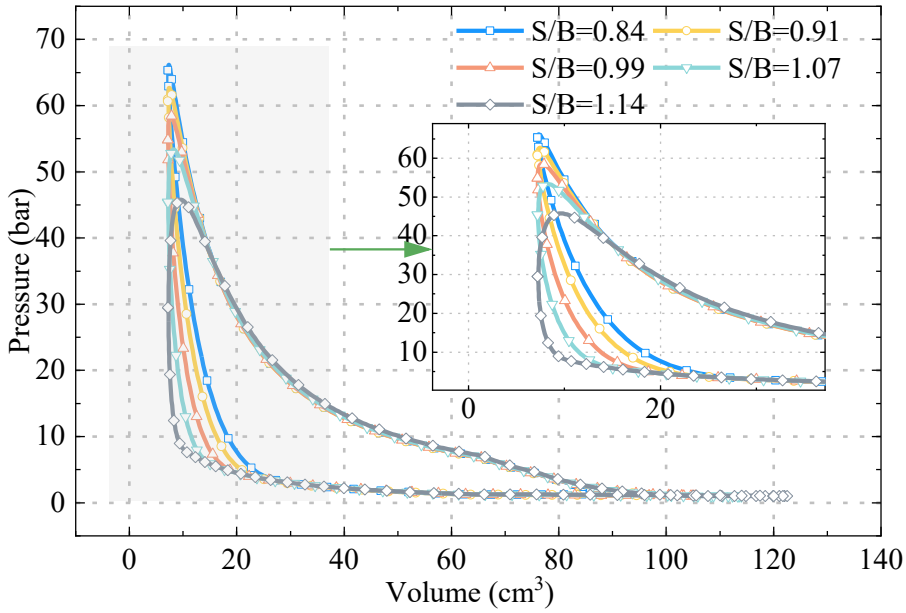

Fig 8. FPEG cylinder pressure at different S/B ratios

The change in cylinder pressure and volume at different S/B ratios are shown in Fig. 8. As can be seen from the P-V diagram, the maximum volume in the cylinder increased with the increase of S/B ratio. Limited by compression ratio, the minimum operating volume of FPEG remained unchanged. Moreover, the lower the S/B ratio, the higher the peak pressure in the cylinder. In order to maintain the same compression ratio at different S/B ratios, the ignition position needs to be adjusted. As the S/B ratio increased, the ignition position increased, so that the FPEG system had the same working compression ratio as shown in Fig. 9, which means that when the engine is ignited, the remaining compression stroke became longer as the ignition position increased. It was found that the higher the S/B ratio, the closer the thermodynamic cycle was to the Otto cycle.

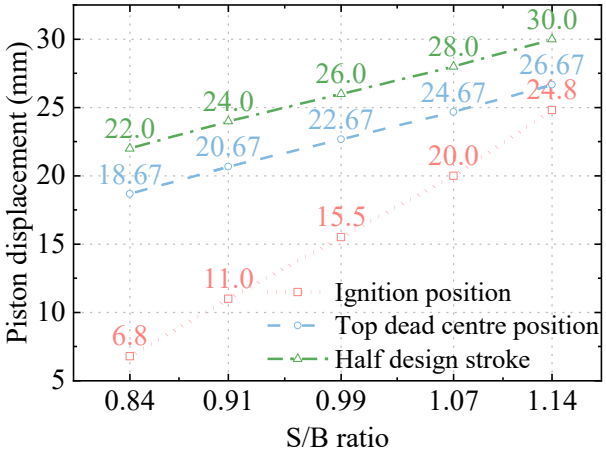

Fig 9. FPEG ignition position with different S/B ratios

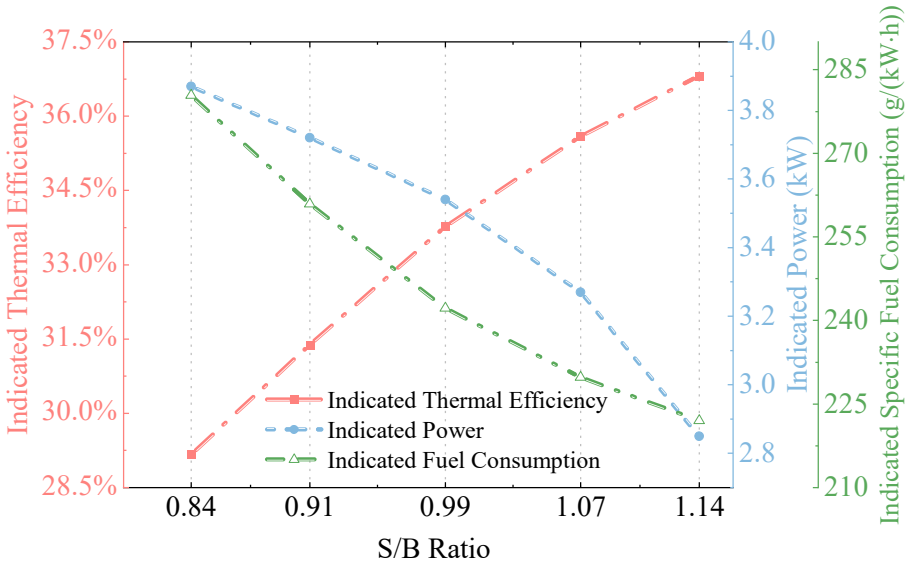

Fig 10. Performance of free piston engine at different S/B ratios

The performance of free piston engine at different S/B ratios is shown in Fig. 10. With the increase of the S/B ratio, the indicated thermal efficiency gradually increased from 29.2% to 36.8%, while the indicated power gradually decreased from 3.9kW to 2.9kW. The reason is that as the S/B ratio increased, the thermodynamic cycle of the free piston engine operation was closer to the Otto cycle, thus improving the thermal efficiency of engine. The indicated thermal efficiency and the indicated power are maintained at a high level when S/B ratio is around 1. However, as shown in Fig. 7, the operating frequency of the system significantly decreased with the increase of S/B ratio, so the working capacity of the gas in the cylinder gradually decreased when the amount of input energy was fixed. As a result, the indicated power output of the free piston engine gradually decreased with the increase of S/B ratio.

4.3 Breakdown of the input energy of the free piston engine at different S/B ratios

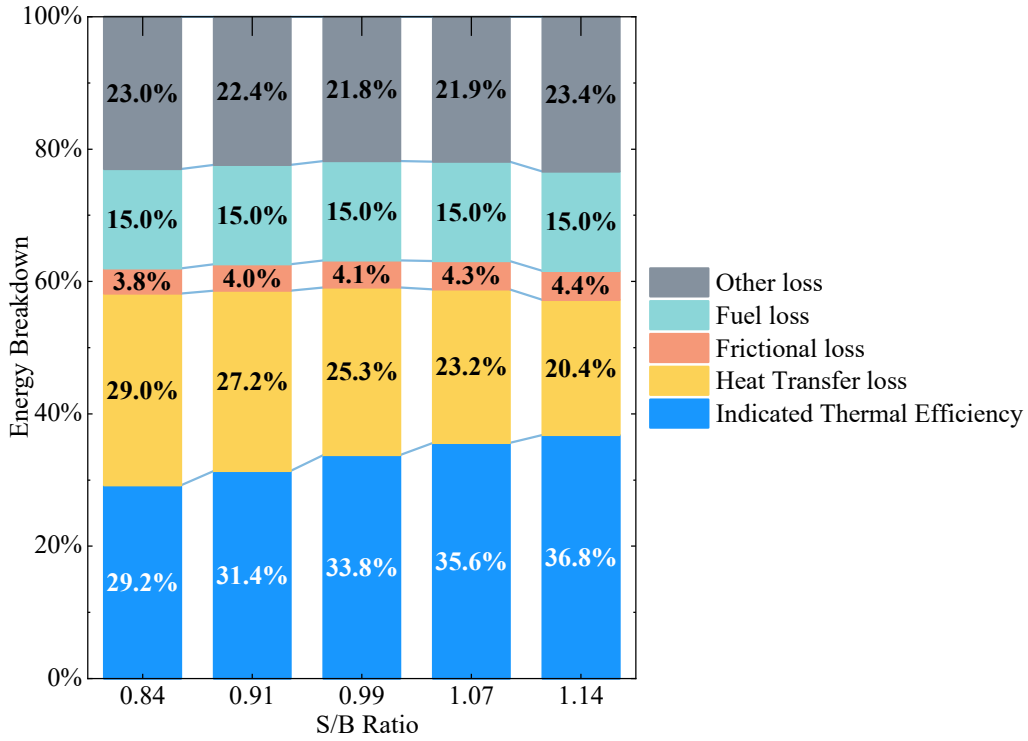

Fig 11. Free piston engine input energy breakdown with different S/B ratios

Fig. 11 shows the free piston engine input energy breakdown with different S/B ratio when the chemical energy input amount is fixed. The combustion efficiency is assumed to be 85% during the simulation, thus the combustion loss is set to 15%. “The other loss” in Fig. 11 includes pump loss and exhaust loss. The frictional loss increases as the S/B ratio increases, as the effective stroke increased. However, the diffidence on frictional loss at different S/B ratios is not significant, and it is found to be less than 5% throughout the simulation, which is considered as much lower than that of a conventional reciprocating engine.

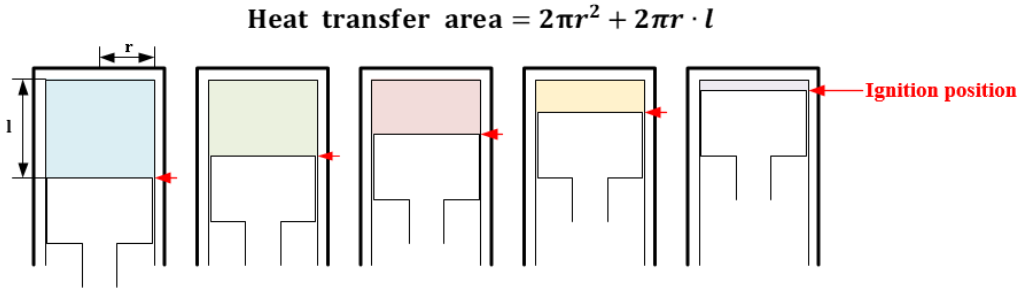

(a) The calculation of heat transfer area

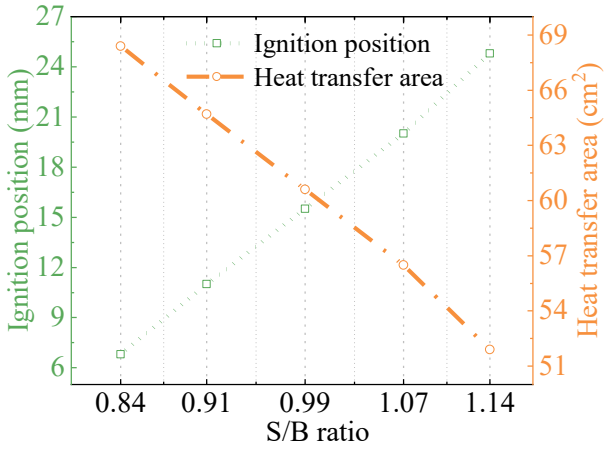

(b) The heat transfer area at ignition position with different S/B ratios

Fig 12. FPEG heat transfer area at ignition position in different S/B ratios

From Fig. 11, the heat transfer loss decreases as the S/B ratio increases. Heat transfer loss is mainly related to heat transfer area and the heat transfer area consists of the cylinder head area, the piston section area and the cylinder wall area as shown in Fig. 12 (a). The ignition position is the distance between the piston position and the geometric centre at the moment of ignition. The results in Fig. 12 (b) showed that the ignition position increases as the S/B ratio increases and the heat transfer area decreases when the ignition position increases. Therefore, the heat transfer loss decreases as the S/B ratio increases.

4.4 System performance with different S/B ratios and different compression ratios

It is difficult to control the free piston engine to operate in one fixed track which means the free piston generally operate under several compression ratios. Therefore, the ideal state of FPEG is running in a small compression ratio range and in this section the performance of FPEG in different S/B ratios and different compression ratios is investigated.

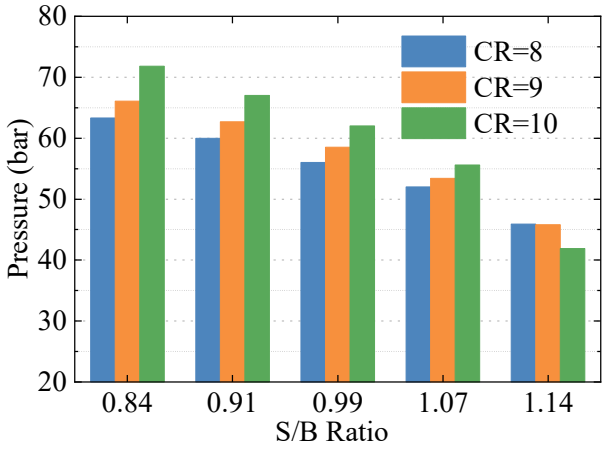

Fig 13. Peak cylinder pressure at different S/B ratios and different compression ratios

In the stable generation process, the change of compression ratio and S/B ratio will also cause the fluctuation of cylinder pressure. The change in the peak in-cylinder pressure of FPEG with different S/B ratios and different compression ratios is shown in Fig. 13. According to the figure, the peak in-cylinder pressure increased with the decrease of S/B ratio, and when the S/B ratio was below 1.07, the peak in-cylinder pressure increased with the increase of compression ratio. However, when the S/B ratio is 1.14, the peak in-cylinder pressure has different behaviour. It is because the difference in ignition position. The ignition position gets closer to the top dead centre as the compression ratio increases as shown in Fig. 14. The effective half stroke should be 27mm when the operation compression ratio is 10 and now the ignition position is 26.5mm. Therefore, after ignition, the free piston engine will soon enter the expansion stroke. The rapid expansion stroke is not conducive to the increase of pressure in the cylinder. As the compression ratio increases, this feature becomes more obvious. It can be seen that the ignition position increased with the increase of S/B ratio and compression ratio. Earlier ignition allows FPEG to work at a lower compression ratio. For FPEG systems with long stroke designs, a further ignition position is required at the same compression ratio as for short stroke designs.

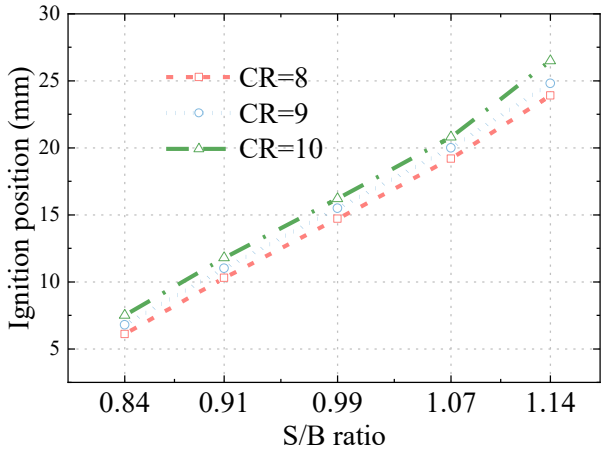

Fig 14. Ignition position of FPEG at different S/B ratios and compression ratios

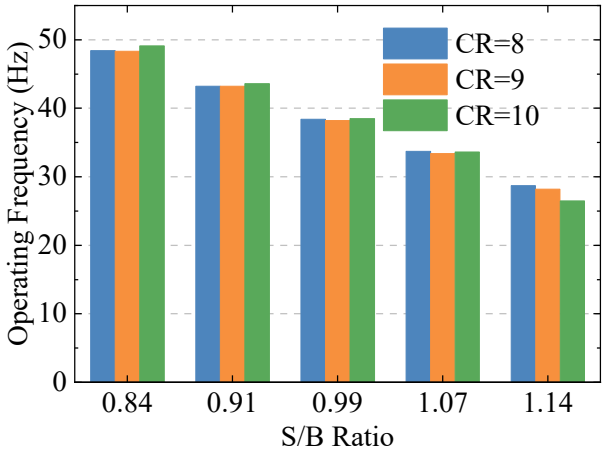

Fig 15. Operating frequency of the system at different S/B ratios and compression ratios

The operating frequency of the system at different S/B ratios and compression ratios are shown in Fig. 15. The results indicate that the operating frequency of the system significantly decreased with the increase of S/B ratio, while the compression ratio had the least influence on the operating frequency of the system. Therefore, in the design process of FPEG, it was found that the short stroke design was beneficial to improve the operating frequency of the system. However, as the compression ratio changed, the operating frequency of the system did not change significantly.

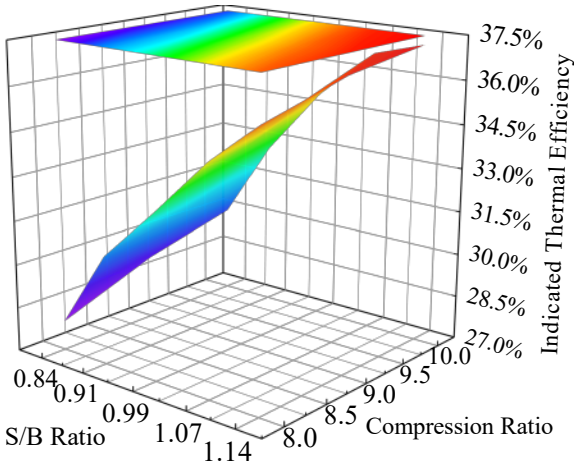

Fig 16. Indicated thermal efficiency at different S/B ratios and compression ratios

The indicated thermal efficiency of the FPEG at different S/B ratios and compression ratios is shown in Fig. 16. With a fixed S/B ratio, the indicated thermal efficiency increased with the compression ratio. When S/B ratio was fixed, the indicated thermal efficiency increased with the increase of compression ratio. Therefore, in determining the design parameters of FPEG and manufacturing the prototype, it is suggested to adjust the ignition timing to make the free piston engine work under high compression ratio to improve the indicated thermal efficiency of the engine. As a result, both high S/B ratio and high compression ratio are required to achieve a high indicated thermal efficiency of the FPEG.

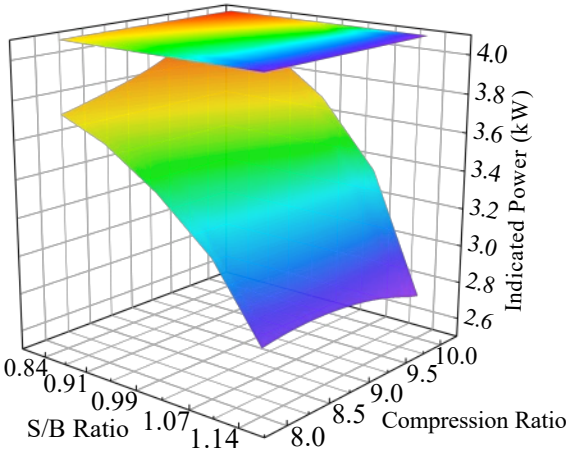

Fig 17. Indicated power of free piston engine at different S/B ratios and compression ratios

The indicated power of engine at different S/B ratios and compression ratios is shown in Fig. 17. The indicated power increased with the increase of compression ratio when

S/B ratio was fixed. When the chemical energy input of FPEG system is constant and the prototype needs higher power output, it is recommended to use lower S/B ratio and run the prototype at a higher compression ratio in the design process of free piston engine.

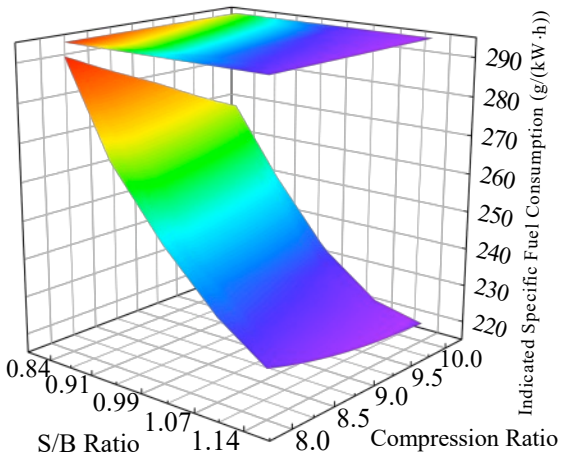

Fig 18. Indicated specific fuel consumption at different S/B ratios and compression ratios

The engine indicated specific fuel consumption is one of the most important parameters to characterize the engine fuel economy. Fig. 18 shows the indicated specific fuel consumption of the designed FPEG system at different S/B ratios and compression ratios. When S/B ratio was constant, the indicated specific fuel consumption decreased with the increase of the compression ratio of engine. The results indicate that long-stroke design and high compression ratio operation are helpful to optimize the fuel economy of the FPEG.

4.5 Discussion

Table 3 The change in the characteristics of FPEG operation with key parameters

Key parameters	Operating frequency	In-cylinder gas pressure	Indicated thermal efficiency	Indicated power	Indicated specific fuel consumption
S/B ratio ↑	↓	↓	↑ ↑	↓ ↓	↓ ↓
CR ↑	—	↑	↑	↑	↓

The influence of S/B ratio and compression ratio on gas pressure, operating frequency, indicated thermal efficiency, indicated power and indicated specific fuel consumption in the cylinder was analysed, and the variation trend is shown in Table 3. The performance of the free piston engine is determined by both the design parameters and the operating parameters. The S/B ratio is one of the most important design parameters and the compression ratio is one of the most important operating parameters. Compared with operating parameters, the influence of design parameters on free piston engine performance is more obvious.

The simulation results will be mainly applied to the optimization design of free piston engines. And combined with the results of comprehensive S/B ratio and compression ratio, it is also of great significance to optimize the operation of free piston engine. Power and thermal efficiency are maintained at a high level when S/B ratio is around 1. On this basis, by increasing the compression ratio of the engine, the power and efficiency of the free piston engine will be further improved. In pursuit of high-power output design, smaller S/B is suggested. And long-stroke design and high operation compression ratio is recommended to improve fuel economy.

5. Conclusion

In this study, the optimal requirement of S/B ratio in the design of FPEG prototype was studied to explore the performance of FPEG in the stable generation process. A numerical model was established in MATLAB/Simulink, and the simulation results were compared with the experimental data obtained from a stable running prototype. The difference between the simulated cylinder pressure and the experimental data could be controlled within 5%, indicating the accuracy of the model.

According to the simulation results, FPEG had a fast expansion stroke and a slow compression stroke, which was more obvious with the increase of S/B ratio. When the working compression ratio was fixed, the difference of piston peak velocity decreased with the change of S/B ratio, but the working frequency decreased with the increase of S/B ratio due to the increase of design and effective stroke.

With the increase of S/B ratio, the indicated thermal efficiency gradually increased, while the indicated power and indicated specific fuel consumption gradually decreased. With the increase of S/B ratio, it can be seen from the P-V diagram that the thermal cycle of FPEG operation was closer to the Otto cycle, but its operating frequency was significantly reduced, suggesting that in the design process of FPEG, the proper S/B ratio should be selected to optimize performance.

The heat transfer loss decreased with the increase of S/B ratio and was mainly affected by the heat transfer area. In order to keep the compression ratio constant, the ignition position increased with the increase of S/B ratio, and the heat transfer area at the beginning of ignition decreased. Under different S/B ratios, the frictional losses accounted for the smallest proportion, all less than 5%.

The in-cylinder pressure decreased from 66.1bar to 45.8bar as S/B ratio increased from 0.84 to 1.14 when the compression ratio is 9. But it decreased as compression ratio increased when the S/B ratio was less than 1.07. Under the influence of ignition position, the variation of pressure in FPEG with long strokes was different. Compression ratio has little effect on working frequency.

It is recommended to adopt high S/B ratio and high compression ratio to achieve high indicated thermal efficiency of FPEG. With the increase of the S/B ratio, the indicated thermal efficiency gradually increased from 29.2% to 36.8%, while the indicated power gradually decreased from 3.9kW to 2.9kW. The indicated specific fuel consumption decreased with the increase of compression ratio, but it decreased with the increase of S/B ratio. In the design process of FPEG, higher S/B ratio will increase indicated thermal efficiency, but will reduce indicated power. And long-stroke design and high compression ratio operation are conducive to fuel economy. The indicated thermal efficiency and the indicated power are maintained at a high level when S/B ratio is around 1. Therefore, the value of S/B should be chosen according to actual needs, taking into account power and economy.

Acknowledgement:

This project is supported by the National Natural Science Foundation of China (project number: 51675043,52005038), and Beijing Institute of Technology Research Fund Program for Young Scholars. The authors would like to thank the sponsors. The authors also thank the Kistler Group for providing us with high measurement accuracy pressure sensors.

References

[1] Mikalsen R, Roskilly AP. A review of free-piston engine history and applications. Applied Thermal Engineering. 2007;27:2339-52.

[2] Hung NB, Lim O. A review of free-piston linear engines. Applied Energy. 2016;178:78-97.

[3] Jia B, Mikalsen R, Smallbone A, Roskilly AP. A study and comparison of frictional losses in free-piston engine and crankshaft engines. Applied Thermal Engineering. 2018;140:217-24.

[4] Jia B, Smallbone A, Zuo Z, Feng H, Roskilly AP. Design and simulation of a two- or four-stroke free-piston engine generator for range extender applications. Energy Conversion and Management. 2016;111:289-98.

[5] Hanipah MR, Mikalsen R, Roskilly AP. Recent commercial free-piston engine developments for automotive applications. Applied Thermal Engineering. 2015;75:493-503.

[6] Van Blarigan P, Paradiso N, Goldsborough S. Homogeneous Charge Compression Ignition with a Free Piston: A New Approach to Ideal Otto Cycle Performance. SAE International; 1998.

[7] Pateras PR. Motor-compressor apparatus. US; 1928.

[8] Pateras PR. Motor compressor of the free piston type. US; 1941.

[9] Rerkpreedapong D. Field Analysis and Design of a Moving Iron Linear Alternator for Use with Linear Engine. Dissertation, West Virginia University. 1999.

[10] Atkinson CM, Petreanu S, Clark N, Atkinson RJ, Famouri P. Numerical Simulation of a Two-Stroke Linear Engine-Alternator Combination. International Congress & Exposition1999.

[11] Houdyschell D. A diesel two-stroke linear engine. Dissertation, West Virginia University. 2000.

[12] Shoukry E, Taylor S, Clark N, Famouri P. Numerical Simulation for Parametric Study of a Two-Stroke Direct Injection Linear Engine. SAE Technical Papers. 2002.

[13] Robinson MC, Clark NN. Study on the Use of Springs in a Dual Free Piston Engine Alternator. SAE International; 2016.

[14] Bade M, Clark NN, Robinson MC, Famouri P. Parametric Investigation of Combustion and Heat Transfer Characteristics of Oscillating Linear Engine Alternator. Journal of combustion. 2018;2018:1-16.

[15] Blarigan PV, Paradiso N, Goldsborough S. Homogeneous Charge Compression Ignition with a Free Piston: A New Approach to Ideal Otto Cycle Performance. SAE Technical Papers. 1998.
[16] Van Blarigan P. Advanced Hydrogen Fueled Internal Combustion Engines. Energy and Fuels. 1998;12:72-7.
[17] Goldsborough SS, Blarigan PV. Optimizing the Scavenging System for a Two-Stroke Cycle, Free Piston Engine for High Efficiency and Low Emissions: A Computational Approach. SAE International. 2003.
[18] Leick, Michael T, Moses, Ronald W. Experimental Evaluation of the Free Piston Engine - Linear Alternator (FPLA). US Department of Energy Technical Report. 2015.
[19] Mikalsen R, Roskilly AP. The design and simulation of a two-stroke free-piston compression ignition engine for electrical power generation. Applied Thermal Engineering. 2008;28:589-600.
[20] Mikalsen R, Roskilly AP. Coupled dynamic–multidimensional modelling of free-piston engine combustion. Applied Energy. 2009;86:89-95.
[21] Mikalsen R, Roskilly AP. The control of a free-piston engine generator. Part 1: Fundamental analyses. Applied Energy. 2010;87:1273-80.
[22] Mikalsen R, Roskilly AP. The control of a free-piston engine generator. Part 2: Engine dynamics and piston motion control. Applied Energy. 2010;87:1281-7.
[23] Mikalsen R, Jones E, Roskilly AP. Predictive piston motion control in a free-piston internal combustion engine. Applied Energy. 2010;87:1722-8.
[24] Mao J, Zuo Z, Feng H. Parameters coupling designation of diesel free-piston linear alternator. Applied Energy. 2011;88:4577-89.
[25] Mao J, Zuo Z, Li W, Feng H. Multi-dimensional scavenging analysis of a free-piston linear alternator based on numerical simulation. Applied Energy. 2011;88:1140-52.
[26] Huihua F, Zhiyuan Z, Boru J, et al. Investigation of the optimum operating condition of a dual piston type free piston engine generator during engine cold start-up process[J]. Applied Thermal Engineering, 2020, 182.
[27] Jia B, Zuo Z, Tian G, Feng H, Roskilly AP. Development and validation of a free-piston engine generator numerical model. Energy Conversion and Management. 2015;91:333-41.
[28] Jia B, Zuo Z, Feng H, Tian G, Roskilly AP. Investigation of the Starting Process of Free-piston Engine Generator by Mechanical Resonance. Energy Procedia. 2014;61:572-7.
[29] Jia B, Tian G, Feng H, Zuo Z, Roskilly AP. An experimental investigation into the starting process of free-piston engine generator. Applied Energy. 2015;157:798-804.
[30] Kosaka H, Akita T, Moriya K, Goto S, Hotta Y, Umeno T, et al. Development of Free Piston Engine Linear Generator System Part 1 - Investigation of Fundamental Characteristics. SAE International; 2014.

[31] Goto S, Moriya K, Kosaka H, Akita T, Hotta Y, Umeno T, et al. Development of Free Piston Engine Linear Generator System Part 2 - Investigation of Control System for Generator. SAE International; 2014.
[32] Moriya K, Goto S, Akita T, Kosaka H, Hotta Y, Nakakita K. Development of Free Piston Engine Linear Generator System Part3 -Novel Control Method of Linear Generator for to Improve Efficiency and Stability. SAE International; 2016.
[33] Siewert RM. Engine Combustion at Large Bore-to-Stroke Ratios. SAE Transactions. 1978;87:3637-51.
[34] Filipi ZS, Assanis DN. The effect of the stroke-to-bore ratio on combustion, heat transfer and efficiency of a homogeneous charge spark ignition engine of given displacement. International Journal of Engine Research. 2000;1:191-208.
[35] Ozcan H, Yamin JAA. Performance and emission characteristics of LPG powered four stroke SI engine under variable stroke length and compression ratio. Energy Conversion and Management. 2008;49:1193-201.
[36] Ikeya K, Takazawa M, Yamada T, Park S, Tagishi R. Thermal Efficiency Enhancement of a Gasoline Engine. SAE International Journal of Engines. 2015;8:1579-86.
[37] Curto-Risso P L , Medina A , A. Calvo Hernández. Optimizing the geometrical parameters of a spark ignition engine: Simulation and theoretical tools[J]. Applied Thermal Engineering, 2011, 31(5):803-810.
[38] Hohenberg Gunter F. Advanced approaches for heat transfer calculations. SAE technical paper, No. 790825; 1979.
[39] Calculation of Blow-by Gas, Lubrication, Friction and Wear in Cylinder Liner-Piston Ring Tribo-Systems. Transactions of Internal Combustion Engine. 1992.

Appendix

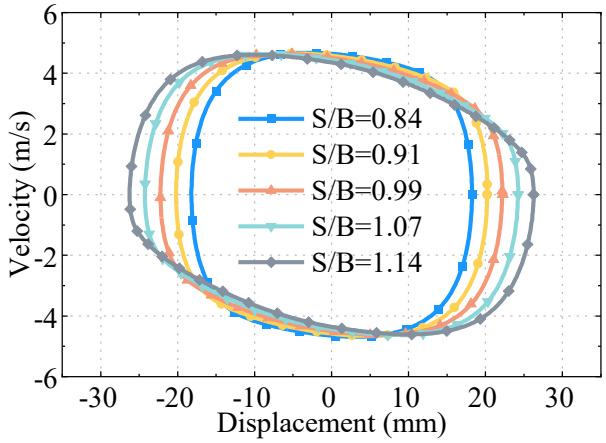

Fig 19. The operating characteristics of FPEG piston at different S/B ratios when the working compression ratio is 8.

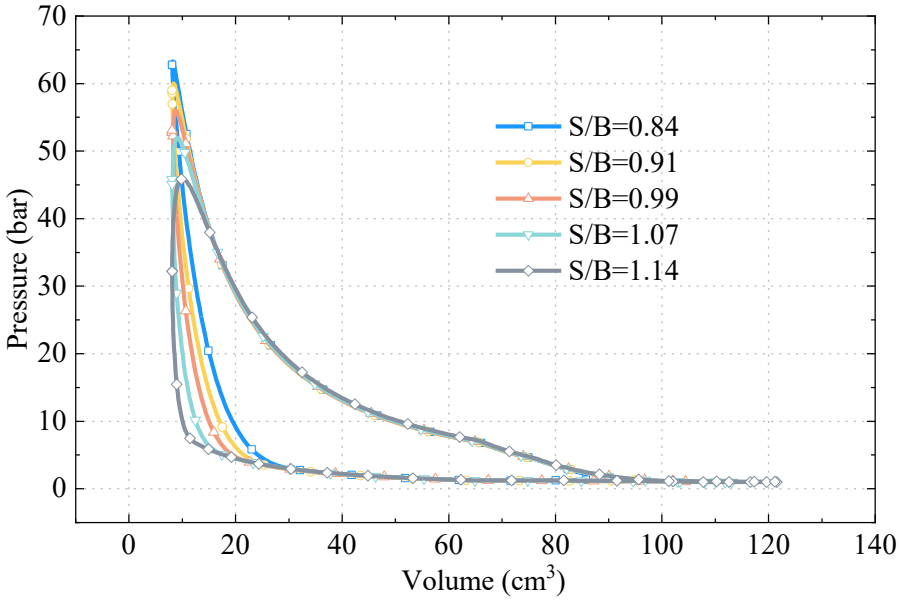

Fig 20. P-V diagram of FPEG at different S/B ratios when the working compression ratio is 8

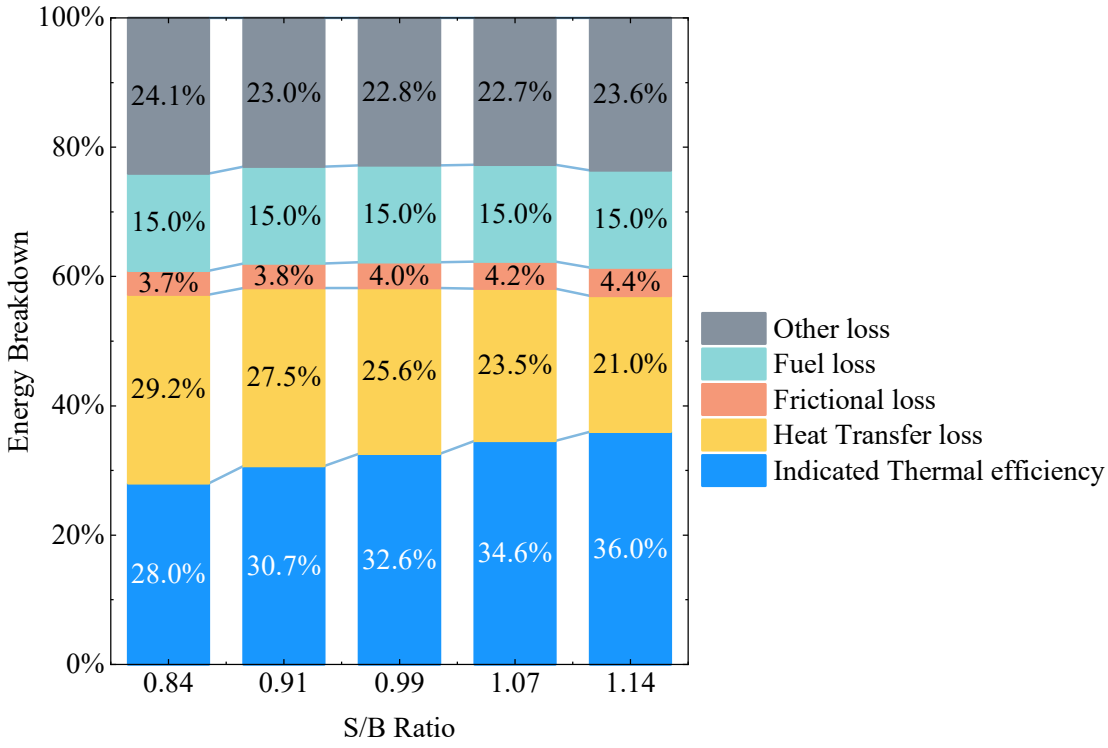

Fig 21. Energy breakdown of FPEG at different S/B ratios when the working compression ratio is 8

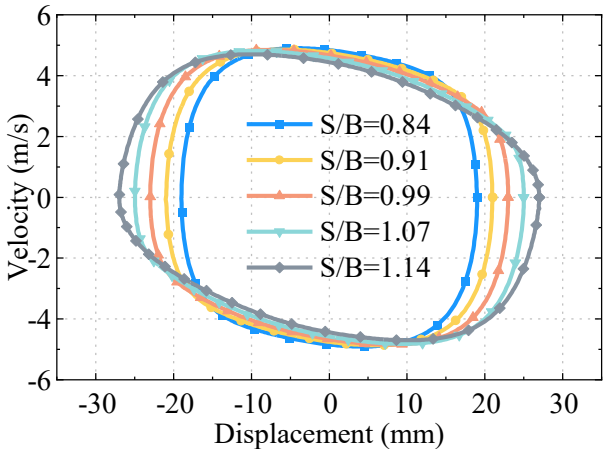

Fig 22. The operating characteristics of FPEG piston at different S/B ratios when the compression ratio is 10

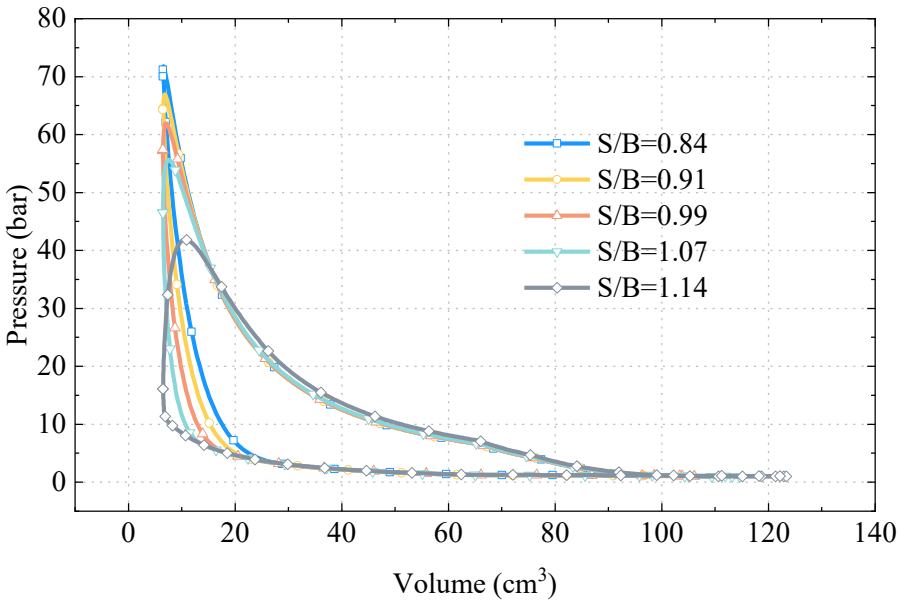

Fig 23. FPEG P-V diagram in different S/B ratios when the operation ratio is 10

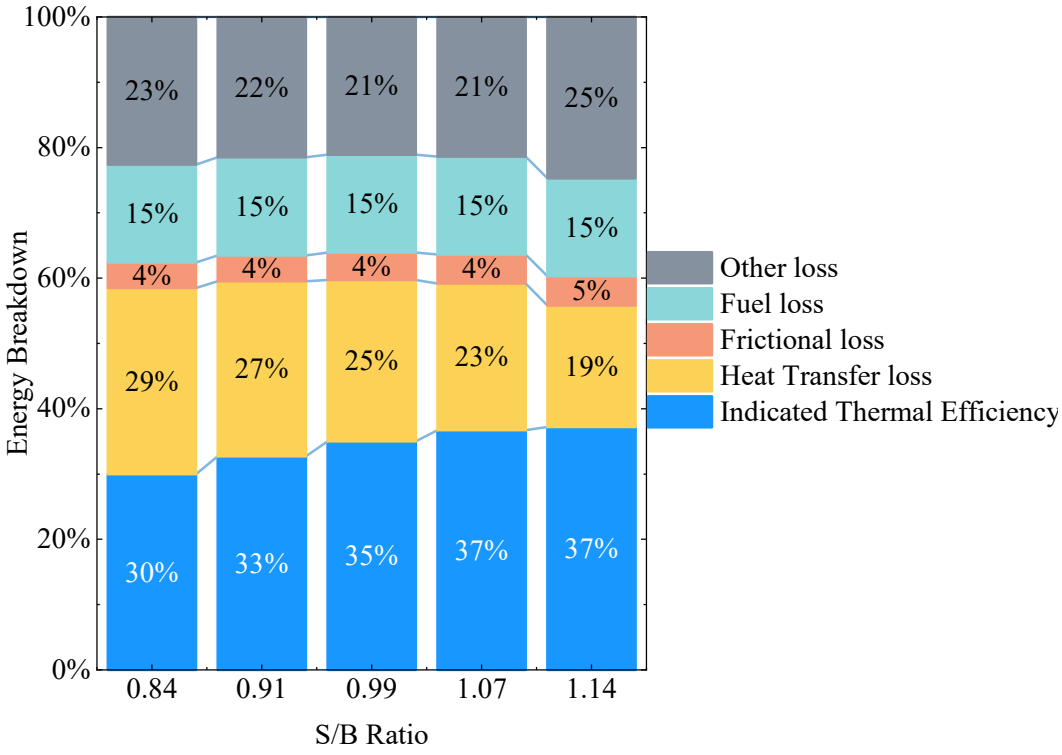

Fig 24. FPEG energy breakdown in different S/B ratios when the operation compression ratio is 10